

# Energy transfer processes on both $\text{Er}^{3+}$ ion concentration and excitation densities in $\text{Yb}^{3+}$ – $\text{Er}^{3+}$ codoped $\text{LaF}_3$ matrix

Jisen Zhang<sup>a</sup>, Weiping Qin<sup>a,b,\*</sup>, Dan Zhao<sup>a</sup>, Gejihu De<sup>a</sup>, Jishuang Zhang<sup>a</sup>,  
Yan Wang<sup>a</sup>, Chunyan Cao<sup>a</sup>

<sup>a</sup>Key Laboratory of Excited State processes, Chinese Academy of Sciences, Changchun Institute of Optical,  
Fine Mechanics and Physics, Changchun 130033, China

<sup>b</sup>State Key Laboratory of Integrated Optoelectronics, College of Electronic Science & Engineering, Jilin University,  
Changchun 130012, China

Received 2 August 2005

Available online 15 February 2006

## Abstract

The effects of both  $\text{Er}^{3+}$  ion concentration and excited density upon frequency upconversion fluorescence emissions in  $\text{Er}^{3+}/\text{Yb}^{3+}$ -codoped  $\text{LaF}_3$  powder are investigated. The results reveal that a higher  $\text{Er}^{3+}$  concentration can induce not only upconversion emission enhancements but also the changes among the relative intensities of the 407, 519, 539 and 651 nm radiation transitions as the samples are excited within the ranges of 20 to 700 mW with 978 nm laser diode (LD) as an excitation source. The changes are described by a schematic level model with the cross-relaxation processes between  $\text{Er}^{3+}$  ions and a series of dynamic equations that take into account the population of temperature dependent in  $\text{Er}^{3+}$ .

© 2006 Elsevier B.V. All rights reserved.

**Keywords:** Upconversion luminescence; Near-ultraviolet luminescence enhancement

## 1. Introduction

So far, miniaturized, practical all solid-state lasers from ultraviolet to green spectral range have

attracted much attention because of a wide range of applications in the fields of high-density optical data storage, all color displays, optical fiber communications, biomedicine and infrared sensors. As one of available approaches in the search for short-wavelength solid-state laser, the effect of frequency upconversion on certain rare-earth ions has been investigated widely in the past two decades [1–10]. For the realization of short-wavelength solid-state lasers, the main drawback is the laser materials themselves.

\*Corresponding author. Key Laboratory of Excited State processes, Chinese Academy of Sciences, Changchun Institute of Optical, Fine Mechanics and Physics, Changchun 130033, China. Tel.: +86 431 6176352, fax: +86 431 4627031.

E-mail addresses: [zhangjisen@yahoo.com.cn](mailto:zhangjisen@yahoo.com.cn) (J. Zhang), [wpqin@public.cc.jl.cn](mailto:wpqin@public.cc.jl.cn) (W. Qin).

$\text{Er}^{3+}$  is the first ion showing upconversion and APTE (sequential two-photons energy transfers) effect has been demonstrated to be a main way for  $\text{Er}^{3+}$  upconversion. With excitation of near-infrared wavelength region, all kinds of upconversion emissions and various energy-transfer processes [11–13] with  $\text{Er}^{3+}$  have been presented and demonstrated. Furthermore, the realization of  $\text{Yb}^{3+}$ -sensitized mechanism has greatly improved upconversion efficiency of  $\text{Yb}^{3+}$ - $\text{Er}^{3+}$  codoped materials [14]. More recently, a detailed review involving  $\text{Er}^{3+}$  on upconversion processes in solid has been reported by Auzel [15]. It can be seen from those that cross-relaxation processes on a single type of  $\text{Er}^{3+}$  ions [16–19] with a more efficient upconversion luminescence have been shown in codoped system. And yet, in converting 978 nm pump radiation to violet and visible light in  $\text{Yb}^{3+}$ - $\text{Er}^{3+}$  codoped  $\text{LaF}_3$  matrix, it is obvious that the energy-transfer processes become complex, and the existing models cannot explain the observed upconversion properties. In order to understand some efficient cross-relaxation processes between  $\text{Er}^{3+}$  ions, we further investigated the influences of the both  $\text{Er}^{3+}$  concentration and the excitation density on the upconversion emissions from  $\text{Yb}^{3+}$ - $\text{Er}^{3+}$  codoped  $\text{LaF}_3$  matrix, and it is observed that the population of  $^4\text{F}_{9/2}$ ,  $^2\text{H}_{11/2}$ ,  $^4\text{S}_{3/2}$  and  $^2\text{H}_{9/2}$  level strongly depends on the both. By ascertaining the role of  $^2\text{H}_{11/2}$  and  $^4\text{S}_{3/2}$  levels in the thermal population processes, a scheme model with the cross-relaxation processes between  $\text{Er}^{3+}$  ions was presented, and the spectral changes were described with a series of dynamic equations that take into account the population variations of  $^2\text{H}_{11/2}$  and  $^4\text{S}_{3/2}$  levels in  $\text{Er}^{3+}$  ions.

## 2. Experimental

The experiment is carried out using  $\text{Er}^{3+}/\text{Yb}^{3+}$ -codoped samples of both  $89.5 \text{ LaF}_3$ - $10 \text{ YbF}_3$ - $0.5 \text{ ErF}_3$  (sample 1) and  $89 \text{ LaF}_3$ - $10 \text{ YbF}_3$ - $1 \text{ ErF}_3$  (sample 2). Two basic samples are synthesized in  $\text{Al}_2\text{O}_3$  crucibles at about  $900^\circ\text{C}$  under a reduced atmosphere and present the thermal stability. Due to the phonon-energy [20] in these materials, it is expected that nonradiative decay rates will be lower. The upconversion spectra is recorded with

F-4500 spectrophotometer and a LD up to 2 W of CW radiation at 980 nm.

## 3. Results and discussion

In this section we will show and discuss the transformation processes of upconversion spectra in a  $\text{Er}^{3+}/\text{Yb}^{3+}$ -codoped  $\text{LaF}_3$  samples.

Fig. 1 shows typical upconversion fluorescence spectra on excitation densities from sample 1. The spectra clearly exhibit the enhancement of the IR to visible upconversion emission as sample 1 is excited from low to high power. By raising  $\text{Er}^{3+}$  concentration, we illustrate the spectral evolution of the upconversion emission from sample 2 at a fixed excitation wavelength 980 nm. From Fig. 2,

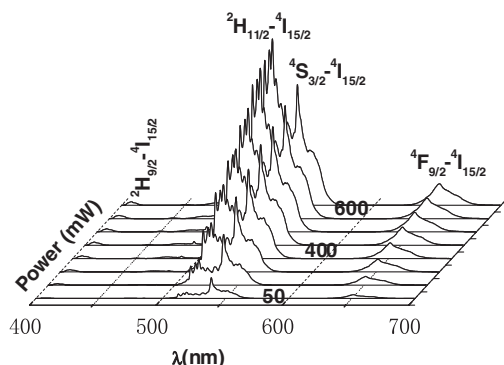


Fig. 1. Upconversion emissions of sample 1 excited at 980 nm from 50 to 600 mW.

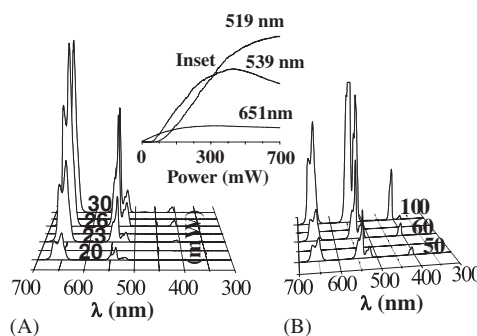


Fig. 2. Upconversion emissions of sample 2 excited at 980 nm from 20 to 100 mW. The inset shows the effects of the excited densities on 651, 539 and 519 nm.

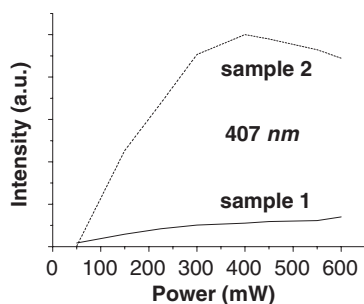


Fig. 3. Near-violet upconversion emission intensity at 407 nm as a function of excited densities.

sample 2 exhibits an upconversion fluorescence spectra different from sample 1. Firstly, the radiation transition from  $^4F_{9/2}$  to  $^4I_{15/2}$  (Fig. 2A) dominates the upconversion spectra under the lower excitation densities; at the higher excitation densities, the spectral pattern (Fig. 2B) evolves into a patent such as that of Fig. 1. From inset of Fig. 2, it can be clearly seen that the green and red upconversion emission changes significantly as the excitation densities vary from 0 to 700 mW. In addition, an enhancement from infrared to the near-ultraviolet upconversion emission at 407 nm has been observed in sample 2. As Fig. 3 shows, up to a ten times near-ultraviolet upconversion emission enhancement at 407 nm has been obtained in this case.

In  $\text{Yb}^{3+}$  and  $\text{Er}^{3+}$  codoped systems, it is well known that excited  $\text{Yb}^{3+}$  firstly transferring its energy into  $^4F_{7/2}$  level of a neighbor  $\text{Er}^{3+}$  ion by APTE processes named after Auzel [15]. From Fig. 1, the intensity of the red upconversion luminescence at 651 nm is always weaker and independent of the excitation densities. This is attributed to the lower non-radiation relaxation rate because of the wider energy gap between  $^4S_{3/2}$  and  $^4F_{9/2}$  or  $^4I_{11/2}$  and  $^4I_{13/2}$  and the lower phonon energies in fluoride matrix. For the weaker near-ultraviolet upconversion emissions, usually, it is due to a lower-efficiency excited-state absorption (ESA) process with the lower transition probability from  $^4F_{7/2}$  to  $^2P_{3/2}$ . So, as described in the energy-level diagram of Fig. 4A, the green upconversion emissions at both 519 and 539 nm are important only in sample 1 with lower  $\text{Er}^{3+}$

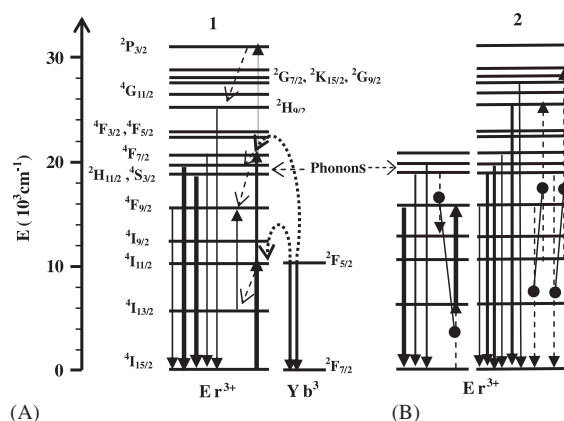


Fig. 4.  $\text{Er}^{3+}$  energy level. A represents case of sample 1, B displays case of sample 2, respectively.

concentration. The increase of  $^2H_{11/2}$  population has recently been reported [21] when a sample is heated from room temperature to 155 °C. It is clear that the phonon-assisted anti-Stokes excitation is responsible for transition from  $^4S_{3/2}$  to  $^2H_{11/2}$ . Therefore, it is possible in our experiment that the sample temperature is raised because of the higher excitation densities, leading to the population change between  $^4S_{3/2}$  and  $^2H_{11/2}$  and the intensity transformation at 519 and 539 nm. However, as can be seen in Fig. 2, the dependence of the upconversion luminescence intensities on the both  $\text{Er}^{3+}$  concentration and the excitation density strongly increases in sample 2, especially, the enhancement at 407 nm implies that there must be a novel upconversion mechanism in sample 2. By comparing the resultant curves indicated in inset of Fig. 2 with Fig. 3, it can be found that the near-ultraviolet enhancement in the direction of the visible light intensity decreases. The experimental results shown in Figs. 2 and 3 are explained by using the energy-level diagram of Fig. 4B and a set of population rate equations of the levels needed to typically describe the model are listed below:

$$\begin{aligned} \dot{n}(^2F_{5/2}) = & n(^2F_{7/2})\sigma(^2F_{7/2}, ^2F_{5/2}) + n(^4I_{11/2})C(^4I_{11/2}, ^2F_{5/2})n(^2F_{7/2}) \\ & - n(^2F_{5/2})C(^2F_{5/2}, ^4I_{15/2})n(^4I_{15/2}) - \frac{n(^2F_{5/2})}{\tau(^2F_{5/2})}, \end{aligned} \quad (1)$$

$$\dot{n}_{(^2F_{7/2})} = n(^2F_{5/2})C_{Yb^{3+}(^2F_{5/2}, ^4I_{11/2})}n(^4I_{11/2}) - \frac{n(^2F_{7/2})}{\tau(^2F_{7/2})}, \quad (2)$$

$$\dot{n}_{(^2H_{11/2})} = n(^2F_{7/2})W_{(^2F_{7/2}, ^2H_{11/2})}^{NR} - \frac{n(^2H_{11/2})}{\tau(^2H_{11/2})(T)}, \quad (3)$$

$$\dot{n}_{(^4S_{3/2})} = n(^2H_{11/2})W_{(^2H_{11/2}, ^4S_{3/2})}^{NR} - \frac{n(^4S_{3/2})}{\tau(^4S_{3/2})(T)}, \quad (4)$$

$$\dot{n}_{(^4F_{9/2})} = n(^4S_{3/2})C_{(^4S_{3/2}, ^4I_{13/2})}n(^4I_{13/2}) + n(^4S_{3/2})W_{(^4S_{3/2}, ^4F_{9/2})}^{NR} - n(^4F_{9/2})C_{(^4F_{9/2}, ^4I_{11/2})}n(^4I_{11/2}) - \frac{n(^4F_{9/2})}{\tau(^4F_{9/2})}, \quad (5)$$

$$\dot{n}_{(^2H_{9/2})} = n(^4F_{9/2})C_{(^4F_{9/2}, ^4I_{11/2})}n(^4I_{11/2}) - \frac{n(^2H_{9/2})}{\tau(^2H_{9/2})}, \quad (6)$$

$$\dot{n}_{(^4I_{11/2})} = n(^2F_{5/2})C_{(^2F_{5/2}, ^4I_{15/2})}n(^4I_{15/2}) + n(^4F_{9/2})C_{(^4F_{9/2}, ^4I_{11/2})}n(^4I_{11/2}) + n(^4S_{3/2})C_{(^4S_{3/2}, ^4I_{11/2})}n(^4I_{11/2}) - \frac{n(^4I_{11/2})}{\tau(^4I_{11/2})}, \quad (7)$$

where  $n_i C_{ij}(n_j C_{ji})$  is the donor (acceptor) energy-transfer rates,  $W_{ij}^{NR}$  is the nonradiative transition probability,  $\tau$  is the level lifetime. In Eqs. (3) and (4), the radiative decay time  $\tau_i(T)$  of the  $^4S_{3/2}$  or  $^2H_{11/2}$  level is temperature dependent. Firstly, the red enhancement at 649 nm (Inset 1 in Fig. 1) can be depicted by an important cross-relaxation process  $(^4S_{3/2} + ^4I_{15/2}) \rightarrow (^4I_{9/2} + ^4I_{13/2})$  under a lower excitation densities. Going with excited power raising, the cross-relaxation process  $(^4F_{9/2} + ^4I_{11/2}) \rightarrow (^4I_{15/2} + ^2H_{9/2})$  induces the saturation of the red emission, and simultaneously, makes  $^2H_{9/2}$  level populated availably and the upconversion luminescence at 407 nm enhanced. When the excitation densities further increase, the increase of  $^2H_{11/2}$  population can be suggested by the transformation of the emission intensities between 519 and 539 nm, and this reduces the cross-relaxation process  $(^4S_{3/2} + ^4I_{15/2}) \rightarrow (^4I_{9/2} + ^4I_{13/2})$  to losing, leading to the obvious decreases of the red and the near-ultraviolet emission.

#### 4. Conclusions

Indeed, the level model and the equations describe quite well our experimental observations for the individual emission intensities at 407, 519, 539, and 651 nm. The temperature variation on the excitation density gives an important contribution to the population changes between  $^4S_{3/2}$  and  $^2H_{11/2}$  levels. We realize that the higher  $Er^{3+}$  concentration is the main reason for the multifold efficiency upconversion emissions with the near-ultraviolet enhancement. In conclusion, the cross-relaxation processes and thermal population of the  $^2H_{11/2}$  level are the dominant reasons of the spectral variations. It is possible for the experimental results to be devoted to the search for all-solid-state blue or near-violet light sources for applications in high-density optical data reading and storage, undersea communications and optical displays.

#### Acknowledgments

The authors would like to thank the support of the National Science Foundation of China (Grant nos. 10274082 and 10474096).

#### References

- [1] M.F. Joubert, Opt. Mater. 11 (1999) 181.
- [2] E. Downing, L. Hesselink, J. Ralston, R. Macfarlane, Science 273 (1996) 1185.
- [3] K. Hirao, S. Tanabe, S. Kishimoto, K. Tamai, N. Soga, J. Non-Cryst. Solids 135 (1991) 90.
- [4] S. Tanabe, K. Tamai, K. Hirao, N. Soga, Phys. Rev. B 53 (1996) 8358.
- [5] A.S. Oliverira, E.A. Gouvias, M.T. De Araujo, A.S. Gouveia-Neto, C.B. de Araujo, Y. Messaddeq, J. Appl. Phys. 87 (2000) 4274.
- [6] W. Ryba-Romanowski, S. Glab, G. Dominiak-Dzik, P. Slarz, T. Lukasmer, Appl. Phys. Lett. 79 (2001) 3026.
- [7] M.P. Hehlen, K. Kramer, H.U. Gudel, R.A. McFarlane, R.N. Schwartz, Phys. Rev. B 49 (1994) 12475.
- [8] R.J. Thrash, L.F. Johnson, J. Opt. Soc. Am. B 11 (1994) 8819.
- [9] B.J. Chen, H.Y. Wang, W.P. Qin, W. Xu, S.H. Huang, Chin. J. Lumin. 21 (2000) 38.
- [10] G.S. Qin, W.P. Qin, et al., J. Appl. Phys. 92 (2002) 6936.
- [11] F. Auzel, Proc. IEEE 61 (1973) 758.
- [12] G.S. Qin, W.P. Qin, C.F. Wu, J.S. Zhang, S.Z. Lu, S.H. Huang, W. Xu, J. Non-Cryst. Solids 347 (2004) 52.

- [13] H.W. Song, B.J. Sun, T. Wang, S.Z. Lu, L.M. Yang, B.J. Chen, X.J. Wang, X.G. Kong, *Solid State Commun.* 132 (2004) 409.
- [14] F. Auzel, F. Pecile, D. Morin, *J. Electrochem. Soc.* 122 (1975) 101.
- [15] F. Auzel, *Chem. Rev.* 104 (2004) 139.
- [16] M. Takahashi, M. Shojiya, R. Kanno, Y. Kawamoto, *J. Appl. Phys.* 81 (1997) 2940.
- [17] V.K. Bogdanov, D.J. Booth, W.W.E.K. Gibbs, *J. Non-Cryst. Solids* 321 (2003) 20.
- [18] L.A. Díaz-Torres, E.D. La Rosa-Cruz, P. Salas, C. Angeles-Chavez, *J. Phys. D* 37 (2004) 2489.
- [19] G.S. Qin, W.P. Qin, S.H. Huang, C.F. Wu, D. Zhao, B.J. Chen, S.Z. Lu, E. Shulin, *J. Appl. Phys.* 92 (2002) 6936.
- [20] F. Auzel, *Rare Earth Spectroscopy*, in: B. Trzebiatowska, J. Legendziewicz, W. Strek (Eds.), World Scientific, Singapore, 1985.
- [21] E.A. Gouveia, M.T. de Araujo, A.S. Gouveia-Neto, *Braz. J. Phys.* 31 (1) (2001) 89.